Static Analysis of V Transmission Lines

Jose E. Schutt-Aine, *Member, IEEE*

Abstract—**In this paper, the v-shaped transmission line is analyzed. The structure consists of a signal strip resting on a dielectric above a triangular reference. A static analysis is performed using the moment method to determine the quasi-TEM propagation parameters. The purpose of this study is to determine the basic electrical properties of the geometry and evaluate the differences from the microstrip configuration. Theoretical results are presented and, in the case of single lines measurements are performed and compare with theoretical predictions.**

I. Introduction

A V-SHAPED transmission line is shown in Fig. 1. The fabrication of v-grooves in silicon is well documented [1]–[5]. The geometry of the transmission line is essentially a microstrip in which the ground plane is bent within the dielectric in a v-shape to form the equal sides, of an isosceles triangle. The triangle as defined by the two ground sides and the dielectric-air interface supports a signal strip of width w on its base. The angle between the two ground sides is the parameter α. The height of the triangle, h, coincides with the dielectric height, and the base of the triangle is $2p$. These geometrical parameters can be used to calculate the electromagnetic properties of the structure.

The bending of the ground plane into a triangular shape is a major deviation from the microstrip structure since the field configuration is significantly modified. From a topological standpoint, the proximity of the ground reference to the signal strip renders a situation similar to that of coplanar waveguides. Several mechanical and electrical advantages are evident such as proximity of ground reference, and in the case of multiple-line structures (see Fig. 2), lower cross-coupling between adjacent lines.

In order to validate the above claims, a static analysis can be performed assuming a quasi-TEM mode of propagation. The calculations would yield parameters that are related to the capacitance and inductance coefficients of the transmission line and which can be determined as a function of the geometrical parameters. An assessment of the propagation properties of the structure can be made from the determination of these parameters. Properties such as characteristic impedance, propagation velocity, and coupling coefficients in the case of multiple lines will be determined and an overall comparison with microstrip will help evaluate the characteristics of this configuration.

Manuscript received June 25, 1991; revised October 25, 1991.

The author is with the Electromagnetic Communication Laboratory, Department of Electrical and Computer Engineering, University of Illinois, 1406 W. Green St., Urbana, IL 61801-2991.

IEEE Log Number 9106043.

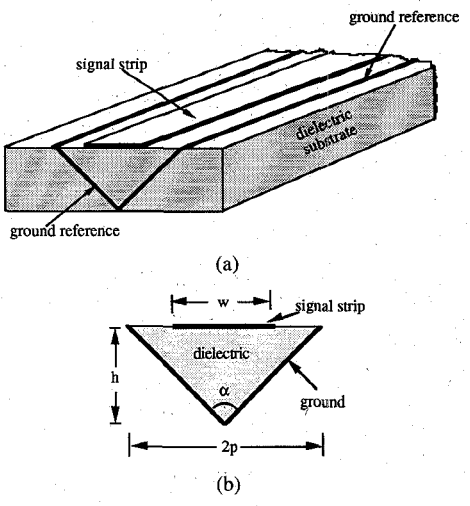

Fig. 1. (a) Transmission line with triangular ground reference. (b) Cross section showing geometrical parameters.

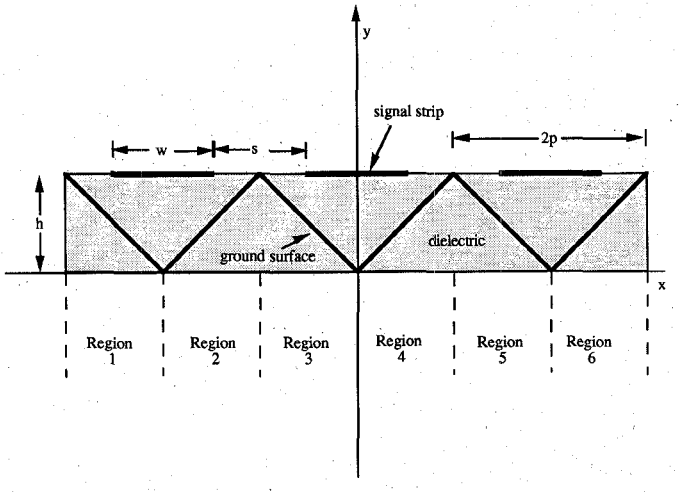

Fig. 2. Cross section of three-line structure with triangular ground reference.

II. Formulation

Static properties of single and coupled microstrip lines have been extensively analyzed in the literature [6]–[15]. These techniques would require substantial revision in order to treat the v-shaped transmission line, thus, a different approach must be adopted. The static formulation is made using the coupled three-line v-strip structure shown in Fig. 2; the method of the analysis would be applicable

for a greater number of lines. Moreover, single-line properties can be deduced from the three-line formulation by making simple reductions. For analytical simplicity, a single quasi-TEM mode of propagation is assumed and the signal strips and ground surface are assumed to be infinitely thin with the signal strips resting at the surface of the dielectric of relative permittivity ϵ_r.

When the coordinate system is chosen as indicated in Fig. 2 and the structure divided into several regions as shown, the relation between the elevation of a point on the conducting strips or ground reference and its horizontal coordinate is given by the general expression

$$y = \frac{shx}{p} + b \tag{1}$$

$s = 1$	ground in regions 2, 4, 6
$s = -1$	ground in regions 1, 3, 5
$s = 0$	top signal strips
$b = 0$	ground in regions 3, 4 and top strips in all regions
$b = +2h$	ground in regions 2, 5
$b = -2h$	ground in regions 1, 6

Since the ground surface is triangular, a Green's function approach that exploits the mirror properties of a perfect electric conductor such as [9], [15] is not amenable in solving for the charge distribution. A more general approach consists of accounting separately for the signal strips and ground reference. Consider an infinitely thin section of surface charge oriented in an arbitrary direction within the dielectric as indicated in Fig. 3. The origin of the coordinate system is placed at a vertical distance h from the air-dielectric interface. The surface charge section is infinite in the z-direction and extends from x_i to x_f in the x-direction and from y_i to y_f in the y-direction. An elemental surface charge located at source point $P'(x', y')$ can be defined. The potential at any observation point within the dielectric $P(x, y)$ due to that elemental surface charge of length dv' is given by [16]

$$d\phi = d\phi_a + d\phi_b \tag{2}$$

$$d\phi_a = \frac{-\sigma}{2\phi\epsilon_r\epsilon_0} \ln \sqrt{(x - x')^2 + (y - y')^2}\, dv' \tag{3}$$

$$d\phi_b = \frac{-\sigma\Gamma}{2\pi\epsilon_r\epsilon_0} \ln \sqrt{(x - x')^2 + (y + y' - 2h)^2}\, dv' \tag{4}$$

where

$$\Gamma = \frac{\epsilon_r - 1}{\epsilon_r + 1}$$

and

$$dv' = \sqrt{1 + \left(\frac{dy'}{dx'}\right)^2}\, dx'$$

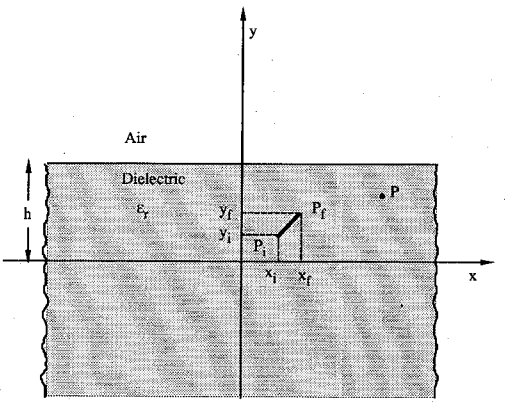

Fig. 3. Cross section showing an infinitely thin surface charge distribution extending from P_i to P_f. P is the observation point where the potential is to be evaluated.

$\sigma = \sigma(x', y', z')$ is the surface charge density at the source point and ϵ_o is the free-space permittivity. It is of interest to note that the contribution $d\phi_b$ is that of a virtual mirror image source located at a point which is oppositely symmetrical to that of the actual source with respect to the air-dielectric interface and of surface charge magnitude $\sigma\Gamma$. The total potential due to the section extending from $P_i(x_i, y_i)$ to $P_f(x_f, y_f)$ is obtained by performing the line integral with respect to the primed coordinates along the section of surface charge. The integration can be performed only if $\sigma(x', y')$ is known; however, if the surface charge section considered is sufficiently short, the charge distribution can be assumed to be uniform over the length and of magnitude σ_o. In that case, the integral can be performed exactly to yield the potential contribution due to that short section:

$$\phi = \sigma_o(F_a + F_b) \tag{5}$$

where

$$F_a = \frac{-1}{2\pi\epsilon_r\epsilon_o}\left[\int_{x_i}^{x_f} \ln \sqrt{(x - x')^2 + (y - y')^2} \cdot \sqrt{1 + \left(\frac{dy'}{dx'}\right)^2}\, dx'\right] \tag{6}$$

$$F_b = \frac{-\Gamma}{2\pi\epsilon_r\epsilon_o}\left[\int_{x_i}^{x_f} \ln \sqrt{(x - x')^2 + (y - y' - 2h)^2} \cdot \sqrt{1 + \left(\frac{dy'}{dx'}\right)^2}\, dx'\right] \tag{7}$$

Using the relations described by (1), y' and dy'/dx' can both be expressed in terms of x'. After extensive algebraic manipulations, the above expressions become

$$F_a = KD(x_f - x_i)\ln(1 + r^2) + KD\left\{(x_f - \xi)\ln[(x_f - \xi)^2 + a^2] - 2(x_f - \xi) + 2a\tan^{-1}\left(\frac{x_f - \xi}{a}\right)\right\} - KD\left\{(x_i - \xi)\ln[(x_i - \xi)^2 + a^2] - 2(x_i - \xi) + 2a\tan^{-1}\left(\frac{x_i - \xi}{a}\right)\right\} \quad (8)$$

$$F_b = KD\Gamma(x_f - x_i)\ln(1 + r^2) + KD\Gamma\left\{(x_f - \xi')\ln[(x_f - \xi')^2 + a'^2] - 2(x_f - \xi') + 2a'\tan^{-1}\left(\frac{x_f - \xi'}{a'}\right)\right\} - KD\Gamma\left\{(x_i - \xi')\ln[(x_i - \xi')^2 + a'^2] - 2(x_i - \xi) + 2a'\tan^{-1}\left(\frac{x_i - \xi'}{a'}\right)\right\} \quad (9)$$

with

$$\xi = \frac{x + \gamma r}{1 + r^2} \quad \xi' = \frac{x - \gamma' r}{1 + r^2} \quad (10a)$$

$$a = \frac{\gamma - xr}{1 + r^2} \quad a' = \frac{\gamma' + xr}{1 + r^2} \quad (10b)$$

$$\gamma = y - b \quad \gamma' = y + b - 2h \quad (10c)$$

$$K = -\frac{1}{2\pi\epsilon} \quad D = \tfrac{1}{2}\sqrt{1 + r^2} \quad (10d)$$

$$r = \frac{sh}{p}. \quad (10e)$$

These expressions represent the basis for the quasi-static formulation. If the geometry (Fig. 2) is divided into several sections, then the total potential at any point can be expressed in terms of the potential contributions from each section. The approximation can be made as accurate as desired since the number of sections can be made arbitrarily large. Up to the present, however, the charge coefficients are unknown; they will be determined using the moment method formulation.

III. Moment Method Solution

The method of moments can be applied to determine the charge coefficients [17]. Each signal strip of the geometry is divided into $N/3$ sections and the ground section is divided into N sections. Each section is assumed to hold a uniform surface charge density; under these conditions, the potential at any observation point can be approximated by

$$\phi = \sum_{k=1}^{N} F_t^{(k)}\sigma_t^{(k)} + \sum_{k=1}^{N} F_g^{(k)}\sigma_g^{(k)}. \quad (11)$$

In the above equation, $F_t^{(k)}$ and $F_g^{(k)}$ are the basis functions associated with the top strips and ground sections, respectively; they are calculated using expressions (8) and (9). $\sigma_t^{(k)}$ and $\sigma_g^{(k)}$ are the coefficients associated with these basis functions; they represent the surface charge densities over the kth strip or ground sections, respectively. In order to apply the moment method, a contour for the integration must be chosen. This contour at which the potential must be known is chosen to be the top strips and the ground surface. Alternatively, the top strips and the triangular surface sections are now the observation points, and a formulation that separates ground and strip potentials now reads

$$\sum_{k=1}^{N}\begin{bmatrix} F_{11}^{(k,m)} & F_{12}^{(k,m)} \\ F_{21}^{(k,m)} & F_{22}^{(k,m)} \end{bmatrix}\begin{bmatrix} \sigma_t^{(k)} \\ \sigma_g^{(k)} \end{bmatrix} = \begin{bmatrix} \phi_t^{(m)} \\ \phi_g^{(m)} \end{bmatrix} \quad (12)$$

where $F_{ij}^{(k,m)}$ is the basis function associated with the potential observed at the mth section of the top strips ($i = 1$) or ground surface ($i = 2$) due to the kth source at the top strips ($j = 1$) or ground section ($j = 2$). $\phi_t^{(m)}$ and $\phi_g^{(m)}$ are the potentials observed at the mth section of the top strips and ground surface, respectively. Since the potential values are known from the strips and since the ground potential is held to zero, the coefficients $\sigma_t^{(k)}$ and $\sigma_g^{(k)}$ associated with this particular arbitrary excitation can be obtained using Galerkin's method in which the test functions are chosen to be the same as the basis functions. Namely for a given set of test functions $F_{ij}^{(q,m)}$, we obtain

$$\begin{bmatrix} F_{11}^{(q,m)} & F_{12}^{(q,m)} \\ F_{21}^{(q,m)} & F_{22}^{(q,m)} \end{bmatrix}\sum_{k=1}^{N}\begin{bmatrix} F_{11}^{(k,m)} & F_{12}^{(k,m)} \\ F_{21}^{(k,m)} & F_{22}^{(k,m)} \end{bmatrix}\begin{bmatrix} \sigma_t^{(k)} \\ \sigma_g^{(k)} \end{bmatrix} = \begin{bmatrix} F_{11}^{(q,m)} & F_{12}^{(q,m)} \\ F_{21}^{(q,m)} & F_{22}^{(q,m)} \end{bmatrix}\begin{bmatrix} \phi_t^{(m)} \\ \phi_g^{(m)} \end{bmatrix}. \quad (13)$$

For each q, ($q = 1$ to N), integration is performed along the contour over the index m [17]; the result yields a $2N \times 2N$ system of equations which can be inverted for the charge coefficients.

IV. Capacitance Calculations

When the charge coefficients are determined, the total charge on each strip is calculated by summing up the coefficients associated with the respective strip

$$Q_i = \sum_k \sigma_t^{(k)} \quad (14)$$

where Q_i is the total charge on the ith strip and the sum is performed over all the sections of that strip. Once the charges on all the strips are obtained, a matrix relation between the total charge on each strip and the voltage V_i (or potential ϕ_i) on the ith strip can be written as

$$\boldsymbol{Q} = \boldsymbol{CV} \quad (15)$$

where Q and V are vectors of dimension 3 representing the charges and voltages on each of the 3 strips, respectively. The coefficient C is a square matrix of order 3 that contains the capacitive coefficients of the structure. To determine C, the moment method problem must be solved with 3 different excitations in order to yield 3 different sets of charge distributions which are then used in (15). The inductance matrix L associated with the geometry can be obtained by removing the dielectric ($\epsilon_r = 1$) and solving for the free-space capacitance matrix C_o which satisfies the relation $L = 1/c^2\, C_o^{-1}$ where c is the free-space propagation velocity.

V. Single-Line Analysis

A moment method program was implemented to calculate the static parameters of single-line and three-line v-strip structures. Basis functions were calculated as per (8) and (9) and the coefficients were determined using the approach described in (13) and (14). Quasi-TEM properties of single lines were first determined. The parameters of interest are the characteristic impedance and the propagation velocity; it can be shown that (8)–(10) can be strictly expressed in terms of the geometrical parameters normalized to h. Therefore, characteristic impedance and propagation velocity will depend on the parameters w/h and α ($= 2 \tan^{-1} p/h$). Plots of the characteristic impedance and the effective relative permittivity values w/h are shown in Figs. 4 and 5 for various values of α. The relative dielectric constant is 2.55. It is of interest to observe the added flexibility obtained over microstrip with the parameter α; in fact the microstrip structure can be considered as a special case of a v line with $\alpha = \pi$. The corresponding curves for a microstrip are also shown; the microstrip characteristic impedance Z_o is substantially higher and, for a fixed w/h, a monotonic decrease in Z_o is observed as α is reduced. This is a result of the ground reference being closer to the signal strip which leads to a significant increase of the capacitance per unit length. An increase of the effective dielectric constant was observed as α was decreased, indicating a greater confinement of the fields within the dielectric whereas the microstrip case showed a lower effective dielectric constant indicating a lower confinement of the fields within the dielectric.

Experimental data were obtained on a sample with height $h = 240$ mils and angle $\alpha = 60°$. The sample was designed by shaving a v insert in a metallic base within which a triangular cross-section of polystyrene material ($\epsilon_r = 2.55$) was inserted. Strips of various widths were placed on top of the dielectric and measured at 1 GHz. The propagation parameters were extracted from the measured scattering parameters using standard transmission-line techniques [18]. Table I shows the characteristic impedance and effective relative permittivity values measured at 1 GHz and a comparison with the associated theoretical static results. Within approximations and experimental errors, the results exhibited good correlations with the theoretical predictions.

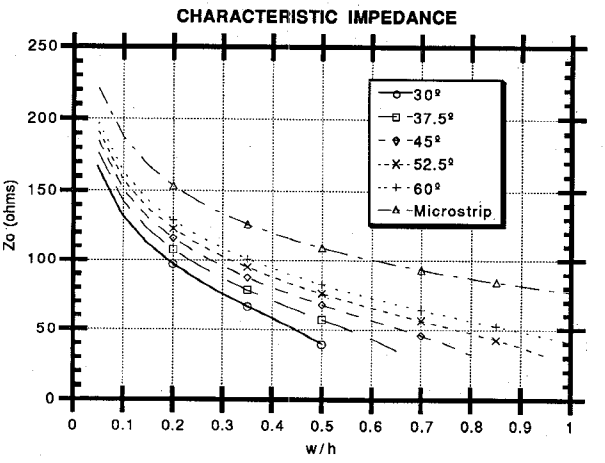

Fig. 4. Calculated values of the characteristic impedance for a single-line v-strip structure as a function of width-to-height ratio w/h and angle α. The relative dielectric constant is $\epsilon_r = 2.55$.

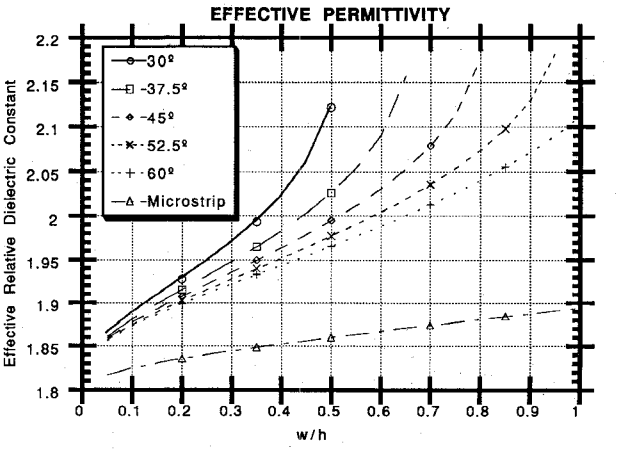

Fig. 5. Calculated values of the effective relative dielectric constant for a single-line v-strip structure as a function of width-to-height ratio w/h and angle α. The relative dielectric constant is $\epsilon_r = 2.55$.

TABLE I
TABLE OF EXPERIMENTAL VALUES FOR THE CHARACTERISTIC IMPEDANCE AND EFFECTIVE RELATIVE PERMITTIVITY MEASURED FOR SINGLE-LINE V-STRIP STRUCTURE OF VARIOUS WIDTH (w) AT 1 GHz

w (mils)	Z_0 (Ω)	ϵ_{eff}
62	107 [115]	1.920 [1.91]
125	76 [78]	1.957 [1.954]

The geometrical parameters are $h = 240$ mils, $\alpha = 60$ degrees. The dielectric material is polystyrene ($\epsilon_r \approx 2.55$). Theoretical values are within brackets.

VI. Coupled-Line Analysis

Theoretical results were also generated for the three-line case. The geometrical parameters, capacitance and inductance matrices generated by the moment method program mentioned in Section V, are shown in Fig. 6 for the structure of Fig. 2. They are compared with those of a microstrip configuration having the same width, height, spacing and dielectric constant. The effect of edge-to-edge

V Line

$$C\ (\text{pF/m}) = \begin{matrix} 74.00 & -0.97 & -0.23 \\ -0.97 & 74.07 & -0.97 \\ -0.23 & -0.97 & 74.00 \end{matrix}$$

$$L\ (\text{nH/m}) = \begin{matrix} 425.84 & 20.35 & 7.00 \\ 20.36 & 422.85 & 20.36 \\ 7.00 & 20.35 & 425.84 \end{matrix}$$

Microstrip Line

$$C\ (\text{pF/m}) = \begin{matrix} 52.49 & -5.90 & -0.57 \\ -5.90 & 53.27 & -5.90 \\ -0.57 & -5.90 & 52.49 \end{matrix}$$

$$L\ (\text{nH/m}) = \begin{matrix} 609.74 & 113.46 & 41.79 \\ 113.54 & 607.67 & 113.54 \\ 41.79 & 113.46 & 609.74 \end{matrix}$$

Fig. 6. Comparison of the inductance and capacitance matrices between a three-line v-line and microstrip structures. The parameters are $p/h = 0.8$ mils, $w/h = 0.6$ and $\epsilon_r = 4.0$.

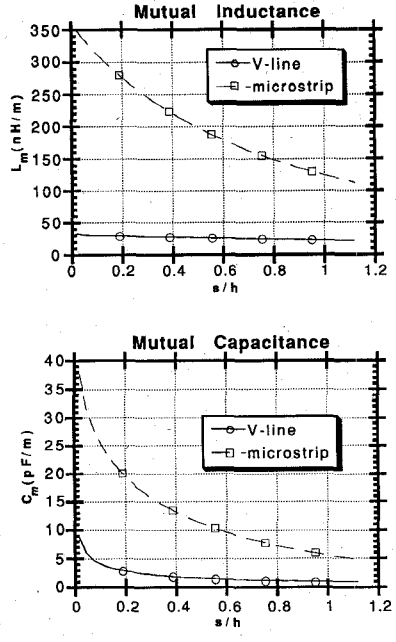

Fig. 7. Plot of mutual inductance (top) and mutual capacitance (bottom) versus spacing-to-height ratio for v-line and microstrip configurations. The parameters are $w/h = 0.24$, $\epsilon_r = 4.0$.

spacing on coupling was also studied. Using the same static moment method program, mutual inductance and capacitance ($L_m = |L_{12}|$ and $C_m = |C_{12}|$) values were plotted as a function of the spacing-to-height ratio s/h. These plots are shown in Figure 7. In both cases, the v-line coefficients were found to be significantly lower. A better measure of the coupling coefficient can be defined [19] as

$$K_v = \frac{Z_{oe} - Z_{od}}{Z_{oe} + Z_{od}} \tag{16}$$

where

$$Z_{oe} = \sqrt{\frac{L_{11} + L_{12}}{C_{11} + C_{12}}} \tag{17}$$

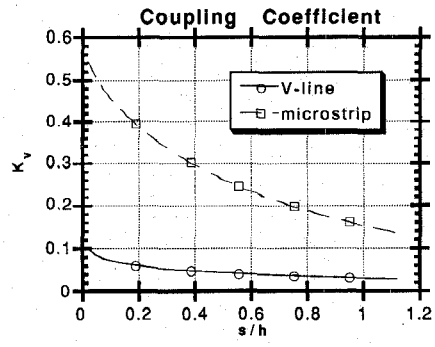

Fig. 8. Plot of the coupling coefficient versus spacing-to-height ratio for v-line and microstrip configurations. The parameters are $w/h = 0.24$, $\epsilon_r = 4.0$.

$$Z_{od} = \sqrt{\frac{L_{11} - L_{12}}{C_{11} - C_{12}}}. \tag{18}$$

For a two-line configuration, Z_{oe} and Z_{od} are equivalent to the even- and odd-mode impedances respectively; K_v is associated with the worst-case crosstalk. Plots of K_v for microstrip and v lines are shown in Figure 8; coupling coefficient is about 5 times larger for microstrip and lower crosstalk levels are achievable with the v line. These results are not unexpected since the v-shaped ground plane provides significant shielding between adjacent lines. Using simulation programs [20], these lower coupling coefficients have been shown to cause reductions in crosstalk by an order of magnitude.

VII. Conclusion

A static analysis of v transmission lines was performed using a moment method formulation. Measurements were performed on a sample and the validity of the theoretical results was verified against experimental data. Characteristic impedance and propagation velocity were found to be strongly dependent on the angle parameter. Comparison with microstrip indicated a lower characteristic impedance and higher effective permittivity for v transmission lines. For multiple lines, the shape of the ground reference led to lower coupling coefficients and lower mutual inductance and capacitance between adjacent lines.

References

[1] K. E. Bean and P. S. Glenn, "The influence of crystal orientation on silicon semiconductor processing," *Proc. IEEE*, vol. 57, pp. 1469–1476, Sept. 1969.

[2] K. E. Bean, "Anisotropic etching of silicon," *IEEE Trans. Electron Devices*, vol. ED-25, no. 10, pp. 1185–1193, Oct. 1978.

[3] I. Adesida and T. E. Everhart, "Substrate thickness considerations in electron beam lithography," *J. Appl. Phys.*, vol. 51, no. 11, Nov. 1980.

[4] E. Bassous, "Fabrication of novel three-dimensional microstructures by the anisotropic etching of (100) and (110) silicon," *IEEE Trans. Electron Devices*, vol. ED-25, no. 10, pp. 1178–1185, Oct. 1978.

[5] E. Bassous and A. C. Lamberti, "High-selective KOH-based etchant for boron-doped silicon structures," *Microelectronics Engineering*, pp. 167–170, 1989.

[6] H. A. Wheeler, "Transmission line properties of parallel wide strips by a conformal mapping approximation," *IEEE Trans. Microwave Theory Tech.*, vol. MTT-12, pp. 280–288, May 1964.

[7] H. A. Wheeler, "Transmission line properties of parallel strips separated by a dielectric sheet," *IEEE Trans. Microwave Theory Tech.*, vol. MTT-13, pp. 172–185, Mar. 1965.
[8] P. Silvester, "TEM wave properties of microstrip transmission lines," *Proc. IEEE*, vol. 115, pp. 43–48, Jan. 1968.
[9] T. G. Bryant and J. A. Weiss, "Parameters of microstrip lines and of coupled pairs of microstrip lines," *IEEE Trans. Microwave Theory Tech.*, vol. MTT-10, pp. 1021–1027, Dec. 1968.
[10] A. Farrar and A. T. Adams, "A potential theory method for covered microstrip," *IEEE Trans. Microwave Theory Tech.*, vol. MTT-21, pp. 494–496, July 1973.
[11] A. Farrar and A. T. Adams, "Characteristic impedance of microstrip by the method of moments," *IEEE Trans. Microwave Theory Tech.*, vol. MTT-18, pp. 65–66, Jan. 1970.
[12] E. Yamashita and R. Mittra, "Variational method for the analysis of microstrip lines," *IEEE Trans. Microwave Theory Tech.*, vol. MTT-16, pp. 251–256, Apr. 1968.
[13] E. Yamashita, "Variational method for the analysis of microstrip-like transmission lines," *IEEE Trans. Microwave Theory Tech.*, vol. MTT-16, pp. 529–539, Aug. 1968.
[14] E. O. Hammerstad, "Equations for microstrip circuit design," in *Proc. European Microwave Conf.*, Hamburg, Germany, Sept. 1975, pp. 268–272.
[15] C. Chan and R. Mittra, "Spectral iterative technique for analyzing multiconductor microstrip lines," in *1984 IEEE MTT-S Int. Microwave Symp. Dig.*, San Francisco, CA, pp. 463–465.
[16] H. Haus and J. R. Melcher, *Electromagnetic Fields and Energy*. Englewood Cliffs, NJ: Prentice-Hall, 1989, pp. 243–244.
[17] R. E. Harrington, *Field Computation by Moment Methods*. New York: Macmillan, 1968.
[18] "Measuring dielectric constant with the HP 8510 network analyzer," *Hewlett-Packard Application Note 8510-3*, Aug. 1985.
[19] H. B. Bakoglu, *Circuits, Interconnections, and Packaging for VLSI*. Reading, MA: Addison-Wesley, 1990, pp. 293–294.
[20] J. E. Schutt-Aine and R. Mittra, "Transient analysis of coupled lossy transmission lines with nonlinear terminations," *IEEE Trans. Circuits Syst.*, vol. CAS-36, pp. 959–967, July 1989.

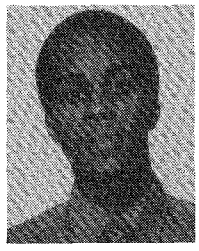

Jose E. Schutt-Aine (M'82) received the B.S. degree from MIT in 1981, and the M.S. and Ph.D. degrees from the University of Illinois in 1984 and 1988, respectively.

Following his graduation from MIT he spent two years with Hewlett-Packard Microwave Technology Center in Santa Rosa, CA, where he worked as a Device Application Engineer. While pursuing his graduate studies at the University of Illinois, he held summer positions at GTE Network Systems in Northlake, IL. He is presently serving on the faculty of the Department of Electrical and Computer Engineering at the University of Illinois as an Assistant Profesosr. Dr. Schutt-Aine's interests include microwave theory and measurements, electromagnetics, high-speed digital circuits, solid-state electronics, circuit design and electronic packaging.